




# Obtaining and main dielectric properties of Ba<sub>0.6</sub>Pb<sub>0.4</sub>TiO<sub>3</sub>/graphene oxide composite

Ryszard Skulski<sup>1,\*</sup> , Dariusz Bochenek<sup>1</sup>, Dagmara Brzezińska<sup>1</sup>, Leszek Stobiński<sup>2</sup>, Przemysław Niemiec<sup>1</sup>, Grzegorz Dercz<sup>1</sup>, and Katarzyna Osińska<sup>1</sup>

<sup>1</sup> Faculty of Science and Technology, Institute of Materials Engineering, University of Silesia in Katowice, 75 Pułku Piechoty Str. 1a, 41-500 Chorzów, Poland

<sup>2</sup> Faculty of Chemical and Process Engineering, Warsaw University of Technology, Waryńskiego 1, 00-645 Warsaw, Poland

Received: 21 September 2020

Accepted: 18 March 2021

Published online:

11 April 2021

© The Author(s) 2021

## ABSTRACT

The paper describes the technology of obtaining and the results of the investigations of microstructure, XRD, SEM, main dielectric properties, electrical conductivity measurements and *P-E* hysteresis loops of Ba<sub>0.6</sub>Pb<sub>0.4</sub>TiO<sub>3</sub>/graphene oxide composite (abbr. BPT/GO). In the final step of the technology, the samples have been sintered using the Spark Plasma Sintering (SPS) method. Diffraction patterns of the BPT/GO composite exhibit lines which can be related to perovskite structure. They also reveal additional lines that can be derived from the initial component oxides. Investigations of electrical conductivity suggest that the positive temperature coefficient of resistivity (PTCR) effect occurs at temperatures up to approximately 120 °C. Dielectric hysteresis loops below 90 °C are wide and typical for materials with rather high electrical conductivity. The hysteresis loop obtained at 120 °C is more typical for ferroelectrics. The obtained material is interesting, nevertheless it is probably possible to find better conditions of obtaining and/or a better composition thereof.

## 1 Introduction

Barium titanate (BaTiO<sub>3</sub>—abbr. BT) is one of the most known ferroelectric material with perovskite structure. Due to the excellent dielectric, piezoelectric and ferroelectric properties thereof, it can be used—for instance—in piezoelectric sensors, multi-layer ceramic capacitors (MLCC), ferroelectric random access memories (FRAM), optoelectronic devices, actuators, and alike. Ferroelectric properties of barium titanate

can be modified by introducing a wide variety of substitutions or dopants into their main structure [1] or even by the addition of second phases to form composite materials [2], which leads to significant changes in the mechanical and dielectric properties.

For some applications, the Curie temperature of BT is too low, therefore solid solutions based on BT are used, for instance Ba<sub>1-x</sub>Pb<sub>x</sub>TiO<sub>3</sub> (BPT). One of the first works concerning BPT was paper [3]. In the solid solution of Ba<sub>1-x</sub>Pb<sub>x</sub>TiO<sub>3</sub>, the Curie temperature

Address correspondence to E-mail: ryszard.skulski@us.edu.pl

linearly decreases from approximately 500 °C for  $x = 1$  to about 120 °C for  $x = 0$ . More recent data on BPT ceramics doped by special glass are presented, for instance, in work [4].

According to work [5], the graphene (G) is a single atomic plane of graphite (GR), which—what is of utmost importance—is sufficiently isolated from its environment to be considered free-standing. Atomic planes are obviously well-known as constituents of bulk crystals, however, a one-atom-thick material such as graphene remained unknown. Graphene is the thinnest known material in the universe and the strongest ever measured.

In the recent years, numerous papers describing the results of the addition of flake Graphene (G) and flake Graphene Oxide (GO) into various materials have been produced, allowing to obtain new composite materials. In general, it provides the new possibilities of changing and improving physicochemical properties. For instance, the introduction of graphene blocks decreases the final grain size. For this reason, the conductivity of the barium titanate/graphene composites does not monotonically increase with carbon content. In work [6], the composites of BaTiO<sub>3</sub>/graphene with different concentrations of the conductive graphene phase have been investigated. In work [6], BaTiO<sub>3</sub>/graphene powders (between 0.1 and 0.6%) have been prepared from BaTiO<sub>3</sub> powders which were dispersed in distilled water and successively mixed with graphene oxide, ball milled and finally sintered using Spark Plasma Sintering (SPS) in vacuum. Finally, it has been exhibited in work [6] that the addition of the graphene blocks the growth of grains of the ceramic matrix, leading to a change of the microstructure at low filler concentrations. As a consequence, the composites exhibit two percolation thresholds and the dielectric properties thereof are not only determined by the dielectric properties of the constituents and their relative fractions, but also by the microstructure of the composite. Finally, grain sizes decrease with the increasing content of graphene.

In work [7], BaTiO<sub>3</sub>/graphene composites were prepared with the wt.% of graphene up to 4%. The temperature dependence and the absolute values of resistivity, as well as the Seebeck coefficient indicate that below 2% the composites behave as n-type semiconductors, whereas over that GO content there is a change towards a more metallic electrical

conduction regime. Concluding, the authors of work [7] stated that ceramic/graphene composites are promising to tailor the thermoelectric power and develop a new thermoelectric material for applications well above room temperature.

Another example of composite material with G and GO can be found in work [8]. The material obtained therein has been prepared for hybrid devices for multi-valued memory system. There are also many other examples of composite materials. For instance, ceramic composites ferroelectric/ferrite [9–11] can be provided.

There are no reports in the literature concerning Ba<sub>1-x</sub>Pb<sub>x</sub>TiO<sub>3</sub>/GO composites. For some applications such material may be interesting.

In this paper, we obtained and described the new ferroelectric-graphene oxide composite material in which as a ferroelectric component, Ba<sub>0.6</sub>Pb<sub>0.4</sub>TiO<sub>3</sub> (BPT) is used. We describe the technology of obtaining and the main physical properties of Ba<sub>0.6</sub>Pb<sub>0.4</sub>TiO<sub>3</sub>/graphene oxide (BPT/GO) composite with 1.6 wt.% of graphene oxide flakes. Such amount of GO flakes has been chosen taking into account results of works [6, 7]. The samples were prepared using a simple processing route starting from Ba<sub>0.6</sub>Pb<sub>0.4</sub>TiO<sub>3</sub> (BPT) powders and an aqueous dispersion of graphene oxide, followed by Spark Plasma Sintering (SPS).

Takeuchi [12] exhibited that SPS applied to BaTiO<sub>3</sub> allows to prepare dense ceramics consisting of sub-micrometre-sized powder. Fixed frequency (1 kHz) measurements revealed that the room temperature permittivity of SPS ceramics was relatively high; approximately double the value of conventionally sintered ceramics. Alternating current (a.c.) impedance spectroscopy measurements shown that SPS is an effective process to reduce the influence of intergranular (grain boundary) effects on the permittivity and direct current (d.c.) resistance characteristics of BaTiO<sub>3</sub> ceramics substantially.

More recently, Niemiec et al. [13] proved that the appropriate selection of all process parameters and sintering conditions during SPS technology are crucial preparing a composite with good properties. Conducting the technology in standard conditions for all materials investigated in work [13] does not improve the physical properties of the PFN–F composite, and further the authors concluded that this requires more in-depth research aimed at the optimization of SPS technology process for composite

ceramic samples. Therefore, it cannot be said how this affects the dielectric properties.

Microstructural studies for BFN ceramics in the work of Bochenek [14] have shown that the use of the SPS sintering allowed to obtain a fine-grained material (but with a heterogeneous shape of grains). SPS technology also changed dielectric properties; for instance sintering with the SPS method resulted in greater frequency dispersion and increased the degree of phase transition diffusion, compared with the FS method. It may be important in practical applications. In general, it cannot easily be said which dielectric properties are better, i.e. whether of the ceramics obtained by FS or of the ceramics obtained by SPS. Of utmost importance is to find the best conditions of SPS (what is not easy because of many parameters).

## 2 Material and methods

The technology of obtaining the BPT/GO composite employed by us was the following. We used commercial powders  $\text{BaTiO}_3$  (Aldrich, purity: 99.9%, grains  $< 5 \mu\text{m}$ ) and  $\text{PbTiO}_3$  (Aldrich, purity: 99%, grains  $< 2 \mu\text{m}$ ). The powders have been weighted and mixed at room temperature, in the proportion of 6/4 (which was supposed to provide the chemical composition  $\text{Ba}_{0.6}\text{Pb}_{0.4}\text{TiO}_3$ ), and then subsequently milled and mixed together with an agate mortar for 2 h. Melting of the oxides was carried out at  $900^\circ\text{C}$ . In the next step, 1.6 wt.% of Graphene Oxide (GO) obtained in the way described in work [15] (Faculty of Chemical and Process Engineering, Warsaw University of Technology, Warsaw) has been added. According to the thermogravimetric analysis [15], at the temperature of  $200^\circ\text{C}$ , graphene oxide GO is almost fully thermally reduced to the form of rGO (reduced Graphene Oxide), decreasing the amount of oxygen groups from approx. 50 wt.% in GO to a few wt.% in rGO. The still remaining oxygen groups, covalently linked to the structure of rGO, are: OH and C=O. In the final step, the composite samples have been sintered using the Spark Plasma Sintering (SPS) method (The Institute of Advancing Manufacturing Technology, Cracow, Poland). The simple and frequently used method of sintering of ceramic materials is the so-called conventional sintering or free sintering (FS). However, in the case of FS method, the relative density usually is low. Spark

plasma sintering (SPS) (as well as hot pressing sintering HP) allows to produce ceramics with fine grains and high density. The dependency of sample temperature as a function of time in SPS process used by us is presented in Fig. 1. The time of holding of the sample at the temperature of approximately  $1000^\circ\text{C}$  is very important since at this temperature during long time rGO is already fully reduced to pure carbon (graphite—GR) [15, 16].

Microstructure and EDS (Energy Dispersive Spectrometry) tests were carried out using a Field Emission Scanning Electron Microscope (Jeol Ltd., JEOL JSM-7100 TTL LV, Tokyo, Japan). Prior to the SEM/EDS analyses, the samples were coated with gold to provide electrical conductivity and to avoid any charging effects.

X-ray measurements for the obtained composite samples were performed using a (PANalytical, Philips X'Pert Pro, Eindhoven, The Netherlands) diffractometer ( $\text{Cu-K}_\alpha$  radiation). The data were collected at room temperature in the  $2\theta$  range from  $10$  to  $80^\circ$ , in the steps of  $0.02$  degrees, with the integration time of  $4$  s/step.

The dielectric measurements were performed using an LCR meter (QuadTech, Inc., 1920 Precision LCR meter, Maynard, MA, USA) during a heating cycle (in temperature range from  $20$  to  $450^\circ\text{C}$ ), at frequencies of the measurement field from  $0.1$  kHz to  $1.0$  MHz.

D.c. electrical conductivity has been measured using an electrometer (Keithley Instruments, Inc.,

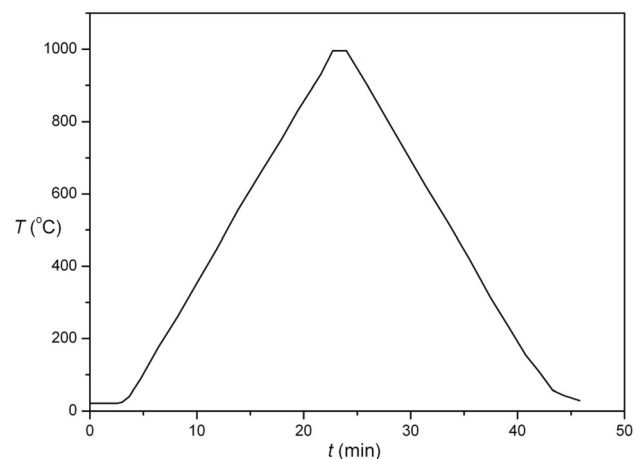


**Fig. 1** The dependency of temperature vs. time during SPS process. Temperature at maximum was equal to  $1000^\circ\text{C}$ , atmosphere argon, pressure  $40$  MPa

6517B, Cleveland, OH, USA), within the temperature range from 20 to 450 °C.

*P-E* ferroelectric hysteresis loops were investigated using a Sawyer-Tower circuit and a high voltage amplifier (Matsusada Precision Inc., HEOPS-5B6, Kusatsu, Japan), in the temperature range from room temperature to 130 °C. The data were stored on a computer disc using an A/D, D/A transducer card (National Instruments) and LabView computer program.

### 3 Results

The measured apparent density of the BPT/GO composite after the SPS process was 6.07 g/cm<sup>3</sup>. For the assumed composition adopting theoretical densities: 6.02 g/cm<sup>3</sup> for BaTiO<sub>3</sub>, 7.52 g/cm<sup>3</sup> for PbTiO<sub>3</sub> and 2.09 g/cm<sup>3</sup> for hexagonal graphite GR, the theoretical density of our sample should be 6.55 g/cm<sup>3</sup>. Therefore, the apparent density measured experimentally is equal to about 93% of the calculated theoretical density.

The analysis of SEM images for the BPT/GO composite with 1.6 wt.% GO for three magnifications is shown in Figs. 2 and 3 (after etching the surface).

It is seen that the grains generally do not have optimal shapes. The grains are heavily fused together, and their breakthrough occurs mainly by seed. However, during cracking, the grains do not disintegrate into small fragments, i.e., their surface is strong and monolithic. It is also seen from Figs. 2 and 3 that the microstructure of the BPT/GO sample is not free from pores; the cracked sample has numerous pores.

An example of the results of EDS analysis of the BPT/GO composite obtained by us is presented in Fig. 4 (in one selected place of the sample).

The EDS investigations of the BPT/GO composite have also been done in ten other locations, and then averaged and compared with the results of the calculations for the assumed composition (Table 1).

It is seen from Table 1 that a large excess of carbon in experimental results occurs. Probably, it can be related with the fact that the graphite matrix has been used during the SPS process. On the other hand, insufficient lead content and excessive barium content can be probably the result evaporation of lead from the sample during sintering. The previously described theoretical value of apparent density at a level lower than expected can be related with this result as well as with a fairly large porosity.

The results of XRD investigations of the BPT/GO composite are shown in Fig. 5. Comparing the obtained diffraction patterns with standards for BaTiO<sub>3</sub>, Ba<sub>4</sub>Ti<sub>13</sub>O<sub>30</sub>, Pb and PbO<sub>2</sub>, as well as with experimental data from work [15] for GO, we can conclude that the most distinct lines correspond to the maxima of BaTiO<sub>3</sub>, while additional maxima correspond to Ba<sub>4</sub>Ti<sub>13</sub>O<sub>30</sub>, Pb and PbO<sub>2</sub>.

During the preparation of the samples for testing of electrical properties, they were cut along the thickness and then polished. Consecutively, the sample was “tempered” by heating at a temperature of 800 °C in the air. After the said operation, the colour of the sample changed from black to light beige. Finally, on both surfaces of the sample, silver paste electrodes were put. Results of the measurement of main dielectric properties vs. temperature are presented in Fig. 6a and b. For this composition of BPT, the maximum of dielectric permittivity ( $\epsilon'$ ) should be

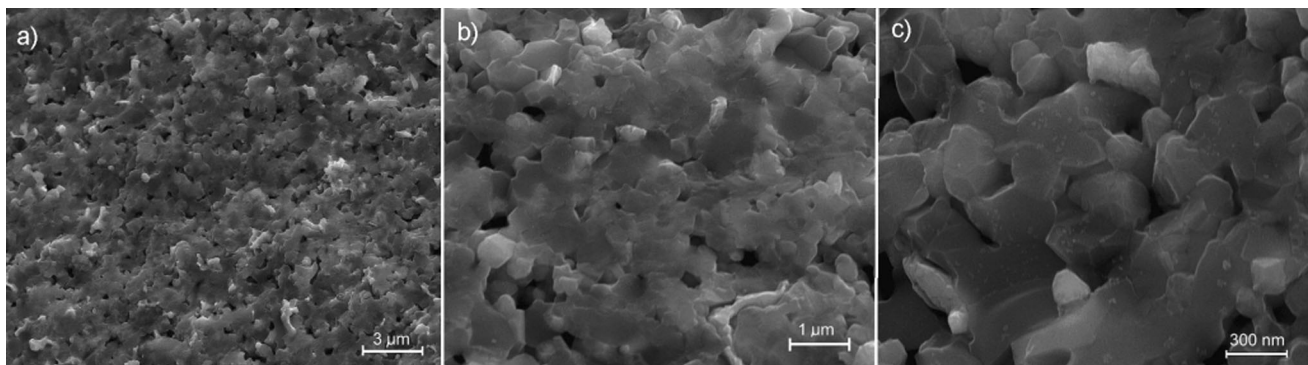


**Fig. 2** FE-SEM images of obtained by us composite BPT/GO with 1.6 wt.% of GO: magnification **a** 5×, **b** 15×, **c** 30×



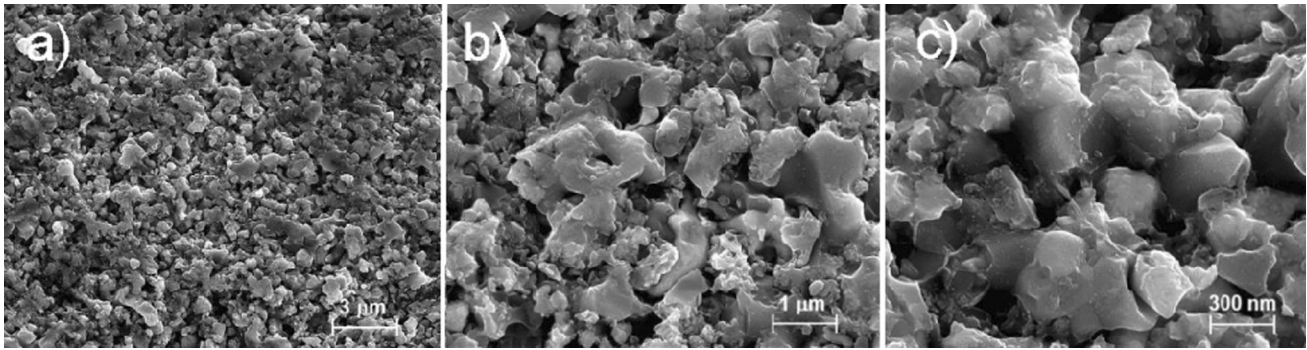


**Fig. 3** FE-SEM images of the composite BPT/GO with 1.6 wt.% of GO after etching the surface: magnification **a** 5×, **b** 15×, **c** 30×

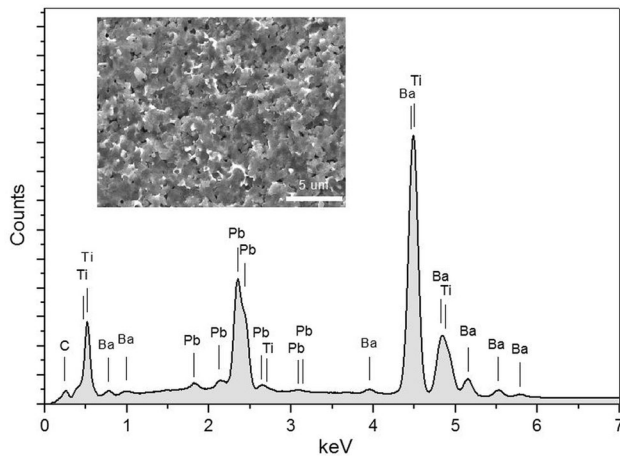


**Fig. 4** The example of EDS spectrum of BPT/GO composite (with 1.6 wt.% of GO)

**Table 1** Results of EDS investigations of the BPT/GO composite obtained in the ten locations and next averaged and compared with calculations for the assumed composition

Symbol of element	Experimental mol % - averaged from 10 locations	Assumed mol %
C	6.11	1.99
O	—	—
Ti	48.00	49.00
Ba	32.75	28.35
Pb	13.15	19.65

observed at temperature 332 °C. Such maximum is seen only for frequencies higher than 10 kHz (see Fig. 6a). For lower frequencies, this maximum is not seen, probably as a result of high electrical conductivity and high dielectric loss (Fig. 6b).

Results of the measurements of main dielectric properties vs. frequency are presented in Fig. 7a and b. Dependencies of  $\epsilon'(f)$  presented in Fig. 7a are rather

typical for normal Deby'e relaxation for samples in which electrical conductivity is important. It is also seen in Fig. 7b, at frequencies below 1 kHz, that the values of  $\tan\delta$  are many times higher than at higher frequencies.

Fig. 8a presents the results of the measurement of d.c. electrical conductivity  $\ln\sigma_{dc}$  vs  $1000/T$ . It is seen from Fig. 8a that the PTCR effect takes place at temperatures up to about 120 °C. In Fig. 8a it is also presented how activations energies  $E_{a1}$  and  $E_{a2}$  have been calculated.

A.c. electrical conductivity has been calculated from dielectric measurements using the formula:

$$\sigma_{a.c.} = \omega \cdot \epsilon_0 \cdot \epsilon' \cdot \tan\delta \tag{1}$$

where  $\omega$  is angular frequency,  $\epsilon_0$  is vacuum permittivity,  $\epsilon'$  is a real part of relative permittivity and  $\tan\delta$  is the loss tangent. Results of the calculations of a.c. electrical conductivity compared with  $\sigma_{dc}$  are presented in Fig. 8b.

The results of the a.c. and d.c. conductivity tests presented in Fig. 8 show that at low temperatures  $\sigma_{ac}$  is higher than the  $\sigma_{dc}$  and increases with the increasing frequency of the measuring field. This is a rather common behaviour for ferroelectric ceramics to which the solid solution of BPT belongs.

The main electro-physical parameters of the obtained BPT/GO composite samples are presented in Table 2.

Results of the investigations of  $P$ - $E$  hysteresis loops are presented in Fig. 9. Hysteresis loops below 90 °C are wide and typical for materials with rather high electrical conductivity. In general, these investigations confirm the fact that from room temperature to about 120 °C, electrical conductivity decreases (PTC effect) and, as a result, the hysteresis loops become more typical for ferroelectrics. The obtained values of

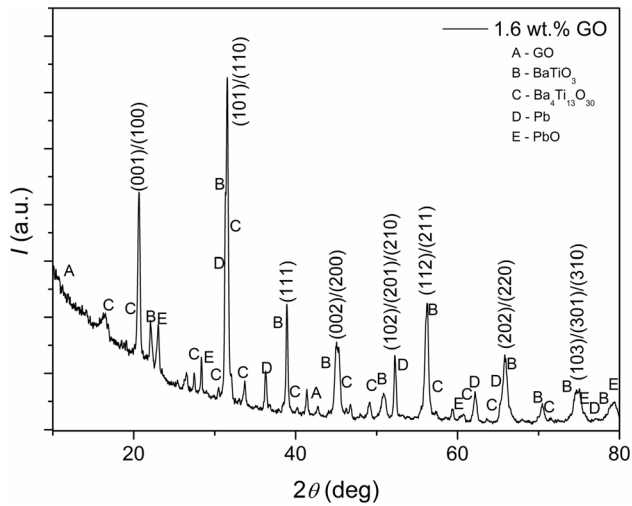


**Fig. 5** XRD pattern of composite sample with 1.6 wt.% of GO. Indexing of maxima is based on comparison with BaTiO<sub>3</sub>

polarization are rather typical for such a type of ferroelectric materials. Investigations at higher temperatures cannot be possible as a result of increasing electrical conductivity with increasing temperature.

## 4 Conclusions

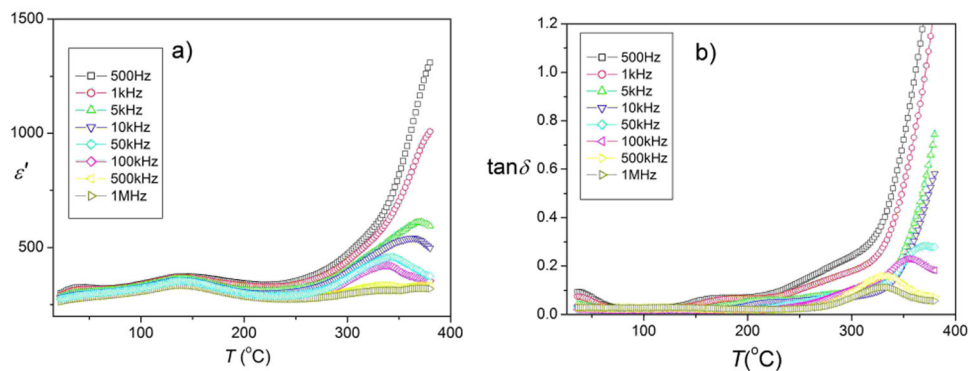
We describe the technology of obtaining and main physical properties of Ba<sub>0.6</sub>Pb<sub>0.4</sub>TiO<sub>3</sub>/graphene oxide (BPT/GO) ceramic composite with 1.6 wt.% of graphene oxide flakes added. In the final step, the samples have been sintered using the Spark Plasma Sintering (SPS) method.

The analysis of SEM microphotographs of the obtained samples shows that the grains are very small and not fully formed. The grains do not have optimal shapes and their breakthrough occurs mainly by seed. However, during cracking the grains do not disintegrate into small fragments, i.e., their surface is strong and monolithic.

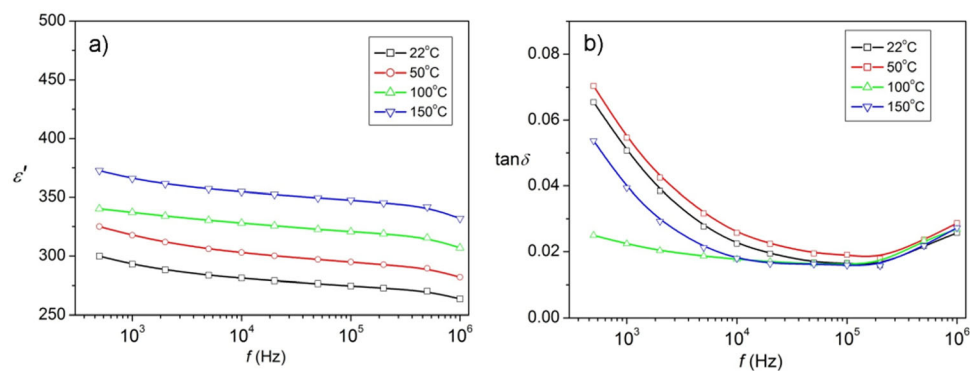
From the investigations of chemical composition using EDS method, we state that it differs insignificantly from the established one. Probably during sintering the evaporation of Pb occurred.

Diffraction patterns of BPT/GO composite exhibit lines which can be related to perovskite structure, as well as additional lines that can be derived from the initial component oxides. However, there are no visible lines either of graphene oxide (GO) or gra-

**Fig. 6** Dependencies  $\epsilon'(T)$  (a) and  $\tan\delta(T)$  (b) for BPT/GO composite sample with 1.6 wt.% of GO



**Fig. 7** Dependencies  $\epsilon'(f)$  (a) and  $\tan\delta(f)$  (b) for BPT/GO composite sample with 1.6 wt.% of GO at various temperatures



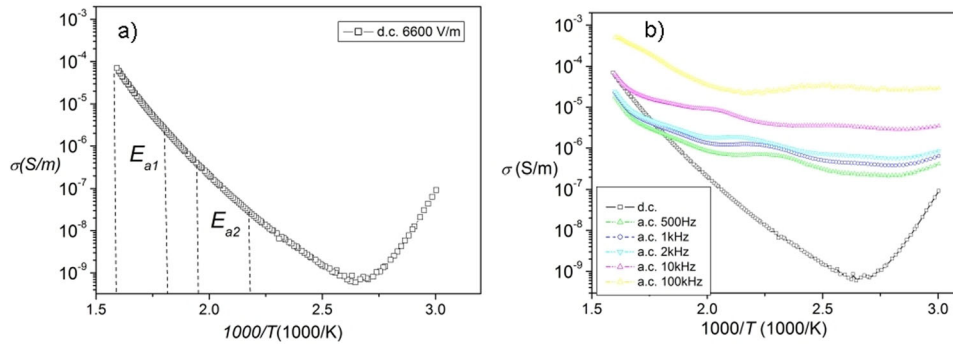


**Fig. 8 a** the result of the measurement of d.c. electrical conductivity  $\ln \sigma_{dc}$  vs  $1000/T$  and explanation activations energies  $E_{a1}$  and  $E_{a2}$  have been calculated **b** dependencies

$\sigma_{dc}(1000/T)$  at constant measuring field 6600 V/m for BPT/GO composite sample compared with dependencies  $\sigma_{ac}(1000/T)$

**Table 2** The electro-physical parameters of the BPT/GO composite samples

$\rho(\text{g/cm}^3)$	$\rho_{theoret}(\text{g/cm}^3)$	$\epsilon_r^{a,b}$	$\tan\delta^{a,b}$	$T_m^b(^\circ\text{C})$	$\epsilon_m$ at $T_m^b$	$\tan\delta$ at $T_m^b$	$E_{a1}(\text{eV})$	$E_{a2}(\text{eV})$
6.07	6.55	293	0.051	386	1026	1.523	1.81	0.967

<sup>a</sup>At room temperature

<sup>b</sup>At 1 kHz

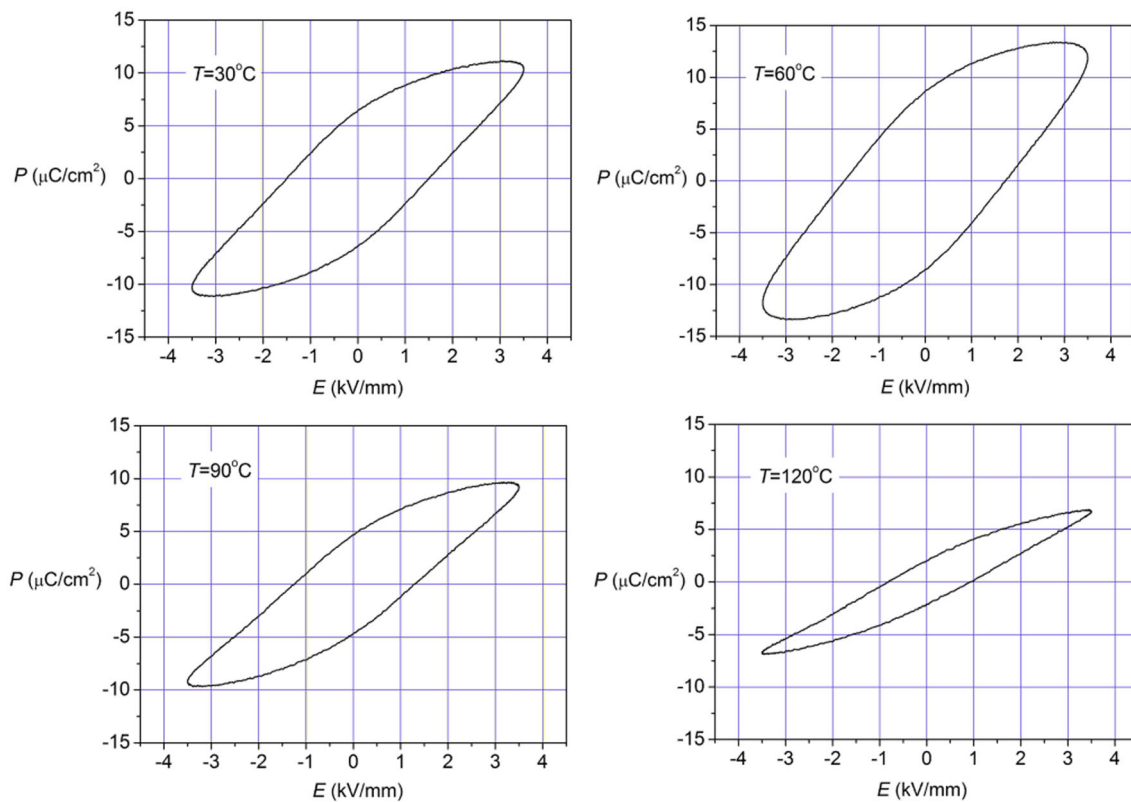


**Fig. 9**  $P$ - $E$  hysteresis loops measured for BPT/GO composite sample with 1.6 wt.% of GO at frequency 1 Hz

phite (GR). The additional phases can be a result of not ideal conditions of SPS process.

The obtained material, up to about 250 °C, has good dielectric properties and low dielectric loss in general, however, the dependencies  $\epsilon'(T)$  and

$\tan\delta(T)$  are rather more complicated than in BT or BPT ceramics. In the temperature range in which the maximum of dielectric permittivity vs temperature occurs, the increase of electric conductivity not allows for precision investigations of Curie-Weiss law.

The values of d.c. conductivity are rather typical for perovskite oxide materials however the dependency  $\ln\sigma_{dc}(1000/T)$  suggests that PTCR effect takes place at temperatures up to about 120 °C. For potential applications in microelectronics, PTCR can be interesting. A similar effect has been found, for instance, in ceramics of solid solutions  $(\text{Pb}_{0.65}\text{Ba}_{0.35})\text{-TiO}_3$  and  $(\text{Pb}_{0.8}\text{Ba}_{0.2})\text{TiO}_3$  [4]. Ferroelectric hysteresis loops below 90 °C are wide and typical for materials with rather high electrical conductivity. The hysteresis loop obtained at 120 °C is more typical for ferroelectric material. It can probably be related to the decrease of electrical conductivity with increasing temperature above 120–150 °C. Therefore, we can state that the obtained material is interesting, however, it is probably possible to find better conditions of obtaining thereof and/or a better composition thereof.

**Open Access** This article is licensed under a Creative Commons Attribution 4.0 International License, which permits use, sharing, adaptation, distribution and reproduction in any medium or format, as long as you give appropriate credit to the original author(s) and the source, provide a link to the Creative Commons licence, and indicate if changes were made. The images or other third party material in this article are included in the article's Creative Commons licence, unless indicated otherwise in a credit line to the material. If material is not included in the article's Creative Commons licence and your intended use is not permitted by statutory regulation or exceeds the permitted use, you will need to obtain permission directly from the copyright holder. To view a copy of this licence, visit <http://creativecommons.org/licenses/by/4.0/>.

## References

1. W. Cai, C. Fu, Z. Lin, X. Deng, *Ceram. Int.* **37**, 3643–3650 (2011)
2. C. Pecharromán, F. Esteban-Betegón, J.F. Bartolomé, S. López-Esteban, J.S. Moya, *Adv. Mater.* **13**, 1541–1544 (2001)
3. S. Nomura, S. Sawada, *J. Phys. Soc. Jpn.* **6**, 36–39 (1951)
4. B. Wodecka-Duś, M. Adamczyk-Habrajska, T. Goryczka, D. Radoszewska, K. Feliksik, L. Kozielski, *Process. Appl. Ceram.* **12**, 129–135 (2018)
5. A.K. Geim, *Science* **324**, 1530–1534 (2009)
6. L. Fernández-García, M. Suárez, J.L. Menéndez, C. Pecharromán, R. Menéndez, R. Santamaría, *Nanoscale Res. Lett.* **10**, 216 (2015)
7. B. Luo, X. Wang, E. Tian, H. Gong, Q. Zhao, Z. Shen, Y. Xu, X. Xiao, L. Longtu Li, *ACS Appl. Mater. Interfaces* **8**, 3340–3348 (2016)
8. S. Jandhyala, G. Mordi, D. Mao, M.W. Ha, M.A. Quevedo-Lopez, B.E. Gnade, J. Kim, *Appl. Phys. Lett.* **103**, 022903–022903–5 (2013)
9. D. Bochenek, P. Niemiec, R. Skulski, A. Chrobak, P. Wawrzala, *Mater. Chem. Phys.* **157**, 116 (2015)
10. D. Bochenek, P. Niemiec, B. Durtka, J. Korzekwa, R. Skulski, *Integr. Ferroelectr.* **173**, 82–88 (2016)
11. D. Bochenek, P. Niemiec, R. Skulski, J. Dercz, *Adv. Sci. Tech.* **98**, 9–14 (2017)
12. T. Takeuchi, E. Bétourné, M. Tabuchi et al., *J. Mater. Sci.* **34**, 917–924 (1999)
13. P. Niemiec, J. Bartkowska, D. Brzezińska, G. Dercz, Z. Stokłosa, *Appl. Phys. A* 126 (2020) Article number: 831
14. D. Bochenek, P. Niemiec, D. Brzezińska, *Arch. Metall. Mater.* **65**(2), 799–804 (2020)
15. L. Stobiński, B. Lesiak, A. Małolepszy, M. Mazurkiewicz, B. Mierzwa, J. Zemek, P. Jiricek, I. Bieloshapka, *J. Electron. Spectrosc. Relat. Phenom.* **195**, 145–154 (2014)
16. L. Stobiński, *Nanomaterials, analysis for flake graphene samples: TGA for GO and rGO.* (Warsaw, Poland), <http://www.nanomaterials.pl/properties>. Accessed 12 March 2021.

**Publisher's Note** Springer Nature remains neutral with regard to jurisdictional claims in published maps and institutional affiliations.